

1 **Infection dynamics of co-transmitted reproductive symbionts are mediated by sex,**
2 **tissue, and development**

3
4 Megan W Jones¹, Laura C Fricke¹, Cody J Thorpe¹, Lauren O Vander Esch¹, Amelia RI
5 Lindsey^{1*}

6
7 *To whom correspondence should be addressed (alindsey@umn.edu)

8 ¹Department of Entomology, University of Minnesota, St. Paul, Minnesota, 55108

9
10
11
12
13
14
15
16
17
18
19
20
21
22
23
24
25
26

27 **ABSTRACT**

28 One of the most prevalent intracellular infections on earth is with *Wolbachia*: a bacterium in the
29 Rickettsiales that infects a range of insects, crustaceans, chelicerates, and nematodes.
30 *Wolbachia* is maternally transmitted to offspring and has profound effects on the reproduction
31 and physiology of its hosts, which can result in reproductive isolation, altered vectorial capacity,
32 mitochondrial sweeps, and even host speciation. Some populations stably harbor multiple
33 *Wolbachia* strains, which can further contribute to reproductive isolation and altered host
34 physiology. However, almost nothing is known about the requirements for multiple intracellular
35 microbes to be stably maintained across generations while they likely compete for space and
36 resources. Here we use a coinfection of two *Wolbachia* strains (“wHa” and “wNo”) in *Drosophila*
37 *simulans* to define the infection and transmission dynamics of an evolutionarily stable double
38 infection. We find that a combination of sex, tissue, and host development contribute to the
39 infection dynamics of the two microbes and that these infections exhibit a degree of niche
40 partitioning across host tissues. wHa is present at a significantly higher titer than wNo in most
41 tissues and developmental stages, but wNo is uniquely dominant in ovaries. Unexpectedly, the
42 ratio of wHa to wNo in embryos does not reflect those observed in the ovaries, indicative of
43 strain-specific transmission dynamics. Understanding how *Wolbachia* strains interact to
44 establish and maintain stable infections has important implications for the development and
45 effective implementation of *Wolbachia*-based vector biocontrol strategies, as well as more
46 broadly defining how cooperation and conflict shape intracellular communities.

47

48 **IMPORTANCE**

49 *Wolbachia* are maternally transmitted intracellular bacteria that manipulate the reproduction and
50 physiology of arthropods, resulting in drastic effects on the fitness, evolution, and even speciation
51 of their hosts. Some hosts naturally harbor multiple strains of *Wolbachia* that are stably
52 transmitted across generations, but almost nothing is known about the factors that limit or promote

53 these co-infections which can have profound effects on the host's biology and evolution, and are
54 under consideration as an insect-management tool. Here we define the infection dynamics of a
55 known stably transmitted double infection in *Drosophila simulans* with an eye towards
56 understanding the patterns of infection that might facilitate compatibility between the two
57 microbes. We find that a combination of sex, tissue, and development all contribute how the
58 coinfection establishes.

59

60 **KEYWORDS**

61 Wolbachia, cytoplasmic incompatibility, symbiosis, vertical transmission, coinfection

62

63 **INTRODUCTION**

64 Eukaryotic cells are home to a diversity of intracellular microbes including mitochondria, plastids,
65 symbionts, and pathogens, many of which are vertically inherited via the maternal germline. The
66 community and interactions between intracellular microbes are associated with diverse effects on
67 host physiology and health. Despite the importance of the intracellular community, little is known
68 about the factors that promote, inhibit, or regulate the establishment and transmission of multiple,
69 coinfecting, intracellular microbes.

70

71 Arthropods are particularly rich in examples of such infections. It is estimated that more than half
72 of arthropods have at least one heritable bacterial symbiont, and ~12% have two or more of these
73 infections (1, 2). The most common of these is an alpha-proteobacterium, *Wolbachia*, a close
74 relative of the intracellular human pathogens *Anaplasma*, *Rickettsia*, and *Ehrlichia* (3). Unlike their
75 close relatives, *Wolbachia* inhabit the cells of arthropods and nematodes, are primarily vertically
76 transmitted via the maternal germline, and alter host physiology and reproduction to facilitate
77 spread through a population (4, 5). Some arthropods stably harbor multiple co-infecting
78 *Wolbachia* strains (6-10), resulting in drastic effects on host fitness, gene flow between

79 populations, horizontal transfer between *Wolbachia*, and even host speciation (8, 10-15). Not only
80 are *Wolbachia* coinfections significant for evolution of both the microbes and the arthropod host,
81 but the increasing interest in establishing secondary *Wolbachia* infections for use in insect control
82 programs necessitates a mechanistic investigation of these intracellular inhabitants (16-18).
83 Previous successes in *Wolbachia*-mediated vector control were more easily attainable because
84 key vector species such as *Aedes aegypti* so happened to naturally lack *Wolbachia* (19, 20).
85 However, many other pest and vector species are already infected with resident *Wolbachia*
86 strains, and establishment of a secondary infection is a potential avenue for control methods (17,
87 18, 21). Furthermore, pathogens and symbionts in related systems are rarely in complete isolation
88 and the intracellular interactions between symbiotic microbes, pathogenic microbes,
89 mitochondria, and viruses can all contribute to altered host physiology, vector competence, and/or
90 clinical progression of disease (22-27).

91
92 While very little is known about the infection dynamics of co-occurring *Wolbachia*, there are
93 several shared characteristics across many of the naturally occurring *Wolbachia* coinfections,
94 indicating there may be shared mechanisms and selective pressures at play. For example, in
95 *Aedes albopictus* infected with *wAlbA* and *wAlbB* *Wolbachia* strains (10), *Nasonia vitripennis* (with
96 *wVitA* and *wVitB* (7)), *Dactylopius coccus* (with *wDacA* and *wDacB* (28)), and *Drosophila simulans*
97 (with *wHa* and *wNo* (12)), each insect has one *Wolbachia* strain from supergroup A and one from
98 supergroup B: perhaps indicating that more divergent strains are more compatible in a co-
99 infection, maybe as a result of niche partitioning. In support of this idea, a recent study describing
100 an artificially generated triple infection of *Wolbachia* strains in *Aedes albopictus* showed there
101 was strong competition between *Wolbachia* from the same supergroup, but not between
102 *Wolbachia* from different supergroups (29). There are other examples of artificially generated
103 multiple infections, but the outcomes are highly variable: sometimes the infection destabilizes and
104 is quickly lost, other times it is stable across many generations (30-35). Ultimately, we do not

105 know which factors facilitate successful establishment and transmission of multiple *Wolbachia*
106 strains within one host matriline.

107

108 There is literature that suggests the titers of individual strains are differentially regulated. In *Aedes*
109 *albopictus* mosquitoes, the native *wAlbB* strain is present at ~6X the titer of the coinfecting native
110 *wAlbA* strain (9). In *Drosophila simulans*, the *wHa* and *wNo* strains establish at different titers in
111 mono-infection conditions, and these titers depend on the combination of strain identity and host
112 tissue (36, 37). However, studies that investigated these strain-specific dynamics leveraged
113 independent fly genetic backgrounds that carried either the *wHa* strain or *wNo* strain, which
114 confounds our interpretation of coinfection dynamics (12, 36-38).

115

116 Broadly, there is evidence for both (1) host control over the titer of individual *Wolbachia* strains,
117 and/or (2) the presence of a coinfecting strain contributing to the regulation of *Wolbachia* density
118 (39, 40). However, we have limited knowledge of (1) how coinfecting strains might establish
119 across host tissues and developmental stages, (2) if coinfecting strains facilitate each other's
120 transmission, (3) if strains evolved to occupy unique niches within the host, (4) if strains go through
121 different severities of population bottleneck from ovary to oocyte, (5) if there are combinatorial
122 effects of the coinfection on host physiology, and ultimately, (6) the host and microbial
123 mechanisms that regulate the maintenance of these coinfections. To begin to investigate these
124 questions, we explore infection and transmission dynamics of multiple vertically inherited
125 intracellular symbionts in a *Drosophila simulans* model which naturally harbors a stable
126 coinfection of two *Wolbachia* strains: *wHa* and *wNo*.

127

128

129

130

131 **METHODS**

132 Bioinformatics

133 Protein sequences from the reference genomes of *wHa* (GCF_000376605.1) and *wNo*
134 (GCF_000376585.1) annotated with PGAP (8, 41) were used to build orthologous groups of
135 *Wolbachia* proteins using ProteinOrtho v5.15 with default parameters (42). Functional annotations
136 were designated with BlastKOALA with (taxonomy group = bacteria) and (database = eukaryotes
137 + prokaryotes) (43). A *Wolbachia* strain phylogeny was reconstructed with FtsZ sequences from
138 A and B supergroup *Wolbachia*, and a D-supergroup *Wolbachia* (*wBm*) as outgroup
139 (Supplemental Table S1). Amino acid sequences were aligned with MAFFT and a simple
140 Neighbor Joining (NJ) algorithm was used to reconstruct relationships including a JTT substitution
141 model and 100 bootstrap replicates (44). Tree topology was visualized in FigTree v.1.4.4
142 (<https://github.com/rambaut/figtree>) prior to annotation in Inkscape v.1.1.2
143 (<https://inkscape.org/>). (44)

144

145 Fly husbandry

146 Fly stocks were maintained on standard Bloomington cornmeal-agar medium (Nutri-fly®
147 Bloomington Formulation) at 25 °C on a 24-hour, 12:12 light:dark cycle under density-controlled
148 conditions and 50% relative humidity. Experiments used the *Drosophila simulans* genome
149 reference line (Cornell Stock Center SKU: 14021-0251.198), originally from Noumea, New
150 Caledonia, which is stably coinfecting with the *wNo* and *wHa* *Wolbachia* strains (12). We
151 generated a *Wolbachia*-free stock with antibiotics for use as a negative control. This stock was
152 generated by tetracycline treatment (20 µg/mL in the fly food for three generations), followed by
153 re-inoculation of the gut microbiome by transfer to bottles that previously harbored male flies from
154 the original stock that had fed and defecated on the media for one week (45). Gonad dissections
155 were performed on live anesthetized flies under sterile conditions, and tissues were immediately
156 flash frozen and stored at -80 °C for later processing. Embryo collections and developmental

157 synchronization was performed using timed 2-hour egg-lays in mating cages on grape agar plates
158 streaked with yeast-paste. For developmental time points, single embryos were collected at two
159 and ten hours, and the remaining embryos were transferred to BSDC media after which single
160 flies were collected as L1, L2, and L3 larvae, white-prepupae, red-eye bald pupae, and pharate
161 males and females (less than two hours post emergence).

162

163 Wolbachia screening

164 Infection status of all stocks was regularly screened with a multiplex PCR assay that produces
165 size-specific amplicons for *wHa* and *wNo* (46). This PCR assay was also used in determining
166 strain segregation during the differential curing experiments (see below). In all cases, DNA was
167 extracted from individual flies with the Monarch® Genomic DNA Purification Kit (New England
168 Biolabs), PCR assays were performed with the strain-specific multiplex primers from (46) and
169 Q5® Hot Start High-Fidelity 2X Master Mix (New England Biolabs) in 20 µl reactions, and products
170 were run on a 1% agarose gel, stained post-electrophoresis with GelRed® (Biotium). For samples
171 that screened negative for *Wolbachia*, DNA integrity was confirmed with PCR using general
172 primers that target arthropod 28S (6). All primer sequences are listed in Table 1.

173

174 Strain specific quantitative PCR (qPCR)

175 To quantify the relative abundance of individual *Wolbachia* strains, we designed *wHa*- and *wNo*-
176 specific qPCR primer sets targeting unique ~100bp amplicons of the *Wolbachia surface protein*
177 (*wsp*). Assay specificity was verified with Sanger sequencing of amplicons, combined with
178 validation against mono-infected samples generated during differential curing (see above). DNA
179 was extracted from flies/tissues with the Monarch® Genomic DNA Purification Kit (New England
180 Biolabs). Strain specific abundance was assessed with the Luna® Universal qPCR Master Mix
181 (New England Biolabs) following manufacturer's instructions, and normalization to host genome
182 abundance via amplification of *rp/32*. All reactions were run in technical triplicate alongside a

183 standard curve and negative controls on an QuantStudio™ 3 Real-Time PCR System (Applied
184 Biosystems™). All primer sequences are listed in Table 1.

185

186 Differential curing of *Wolbachia* strains

187 To disrupt coinfection transmission, we designed a partial heat-cure to reduce *Wolbachia* titers
188 and increase the severity of the bottleneck as *Wolbachia* are deposited in each embryo. Bottles
189 of ~200 *Drosophila simulans* were kept at 30 °C for four days (or at 25 °C as a control), after
190 which flies were transferred to fresh media under standard rearing conditions (see above) and
191 allowed to oviposit for three days. Offspring (adults <24 hours post eclosion) of the heat-treated
192 mothers were collected and stored in ethanol for further processing.

193

194 Statistics and Data Visualization

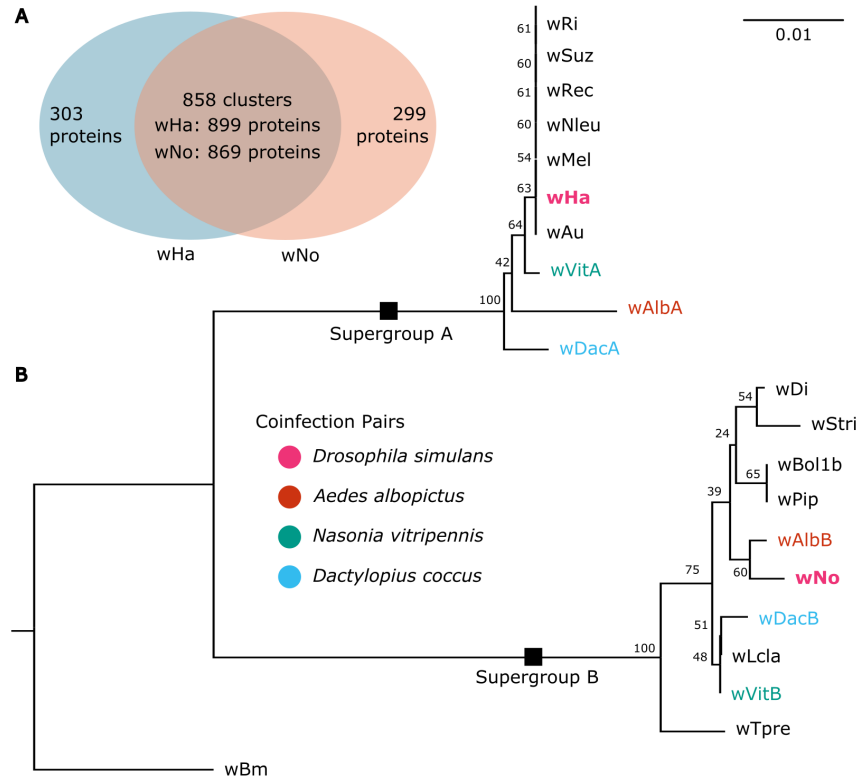
195 All statistics and data visualization were carried out in R version 3.5.0 (47). We used permutational
196 multivariate analysis of variance with the adonis function from the vegan package (48) to assess
197 variation in coinfection titers (a multivariate response) across fly samples using Euclidean
198 distance and 1,000 permutations. Fixed effects were specific to each experimental analysis and
199 included: sex, mating status, and the interaction of the two (Figure 2A), tissue, sex, and the
200 interaction of the two (Figure 2B), or developmental stage (Figure 3). Pairwise comparisons were
201 performed with a Mann-Whitney U test (function “wilcox.test”) followed by Bonferroni Corrections
202 in the case of multiple testing. In the case of the mated vs unmated ovary samples (Figure 4A),
203 we were interested in strain-specific dynamics upon mating, so we assessed variation in strain
204 titers with a two-way ANOVA (function “aov”) including “strain” and “mated status”, along with their
205 interaction, as fixed effects. Correlation between abundance of strains or between abundance in
206 different tissues was assessed with a Spearman’s rank correlation for the data in Figure 2
207 (function “cor.test”, method= “spearman”). Linear regression was performed with the “lm” function.

208

209 **RESULTS**

210 Coinfecting strains wHa and wNo share 75% of their coding sequences

211 To better understand the factors that might facilitate compatibility of two strains we used a suite
212 of bioinformatic approaches to look at phylogenetic and genomic patterns of *Wolbachia*
213 coinfections. Our focal strains, wHa and wNo (from supergroup A and B, respectively) that
214 coinfect some populations of *Drosophila simulans*, share 858 orthologous groups of proteins,
215 approximately 75% of the coding content of each strain (Figure 1A). The remaining ~300 proteins
216 in each strain that are not shared are largely hypothetical, unannotated protein sequences, and
217 only 10-15% were assigned a putative function (wHa n = 31/303; wNo = 44/299). Annotated
218 proteins (i.e., assigned a KEGG KO term) specific to wNo included 16 transposases, 15 proteins
219 that were related to transcription, DNA repair, or endonuclease activity, and the remaining were
220 largely metabolic in predicted function (Supplemental Table S2). Notably, wNo encodes for a
221 putative multidrug efflux pump that is not present in wHa. wHa-specific proteins included 15
222 transposases, three proteins predicted to be involved in transcription or DNA repair, and then a
223 suite of proteins mostly with predicted functions in amino acid transport and metabolism.
224 Interestingly, the wHa strain has two proteins for an addiction module toxin (RelE/StbE family),
225 and a predicted eukaryotic-like golgin-family protein, potentially an effector protein that could
226 interact with host intracellular membranes.



227

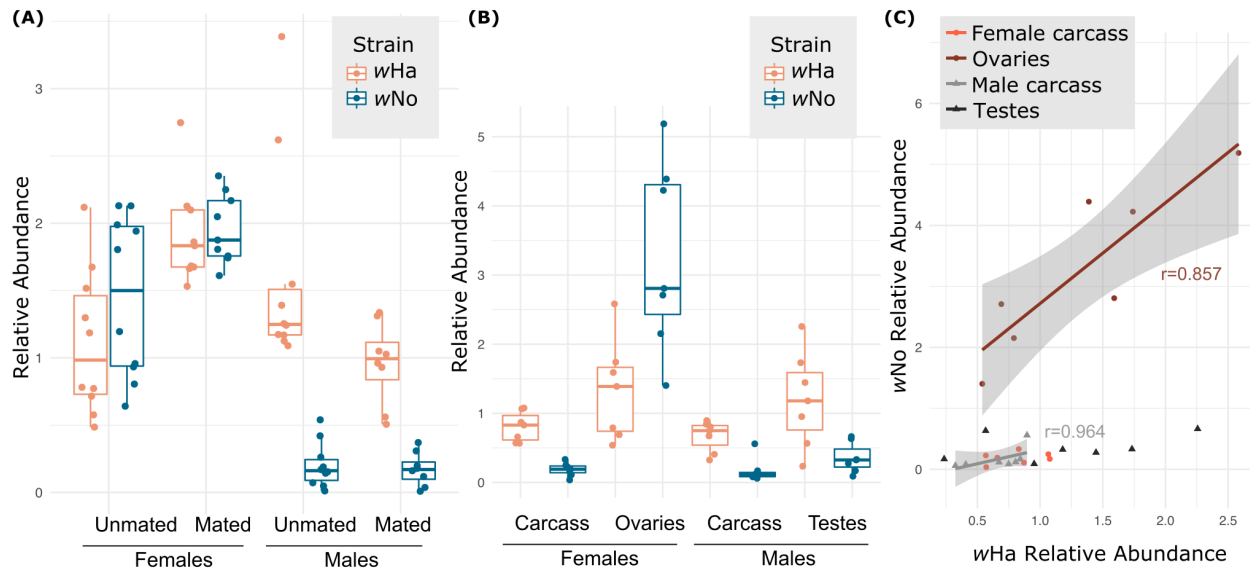
228 **Figure 1. Coinfecting *Wolbachia* strains. (A)** Shared and unique genes between the focal
 229 strains *wHa* and *wNo* that coinfect *Drosophila simulans*. **(B)** Phylogenetic reconstruction of A-
 230 and B- supergroup *Wolbachia* based on FtsZ protein sequences, with colors indicating pairs of
 231 *Wolbachia* strains that can be found together within a given host. Node labels indicate bootstrap
 232 support (n = 100 replicates).

233

234 Strain-specific titers are sex dependent

235 We assessed the titers of the *wHa* and *wNo* strains in whole body three-day old unmated males
 236 and females, and three-day old males and females 24 hours post mating (Figure 2A). There was
 237 a significant effect of the interaction between fly sex and mated status ($F_{1,33} = 4.076$, $p = 0.033$)
 238 as well as a significant effect of sex alone ($F_{1,33} = 69.568$, $p = 0.001$), but not of mated status alone
 239 ($F_{1,33} = 0.488$, $p = 0.500$). This was seen as relatively equal titers of *wHa* and *wNo* in female flies
 240 that slightly increased in total abundance upon mating. In contrast, males had drastically reduced

241 titers of *wNo*, both relative to *wNo* in females, and relative to the coinfecting *wHa* stain within a
242 male. *wHa* titers were slightly reduced in males upon mating. Together, these data indicate strong
243 sex-dependent effects on coinfection dynamics.



244 **Figure 2. Infection densities of coinfecting *Wolbachia* strains.** (A) *wHa* and *wNo* titers in
245 whole body mated and unmated males and females. There was a significant effect of the
246 interaction between fly sex and mated status ($F_{1,33} = 4.076$, $p = 0.033$) and sex ($F_{1,33} = 69.568$, p
247 $= 0.001$) on the coinfection. (B) *wHa* and *wNo* titers of gonads and carcasses of unmated males
248 and females. The interaction of sex and tissue significantly affected the coinfection ($F_{1,27} = 19.334$,
249 $p = 0.001$), as well as sex alone and tissue alone ($F_{1,27} = 19.982$, $p = 0.001$, and, $F_{1,27} = 27.147$, p
250 $= 0.001$, respectively). (C) Correlation between *wHa* and *wNo* abundance within each sample.
251 Regression lines are shown for ovaries and male carcasses, for which we identified significant
252 correlations in strain-specific abundance (see main text).
253

254 Coinfection dynamics are sex and tissue dependent

256 A subset of the unmated males and females were dissected prior to DNA extraction resulting in
257 paired gonadal and “carcass” (all remaining tissue) samples for each fly. Strain specific qPCR
258 revealed that the interaction of sex and tissue identity had a significant effect on the abundance

259 of the two strains in the coinfection ($F_{1,27} = 19.334$, $p = 0.001$). Additionally, there was significant
260 effect of sex alone, and tissue alone ($F_{1,27} = 19.982$, $p = 0.001$, and, $F_{1,27} = 27.147$, $p = 0.001$,
261 respectively). In contrast to the relatively equal titers of *wHa* and *wNo* seen in whole female
262 samples (Figure 2A), we found that ovaries were highly enriched for the *wNo* strain (Figure 2B).
263 However, in all other sample types (female carcasses, male testes, male carcasses), the *wHa*
264 strain was significantly more abundant.

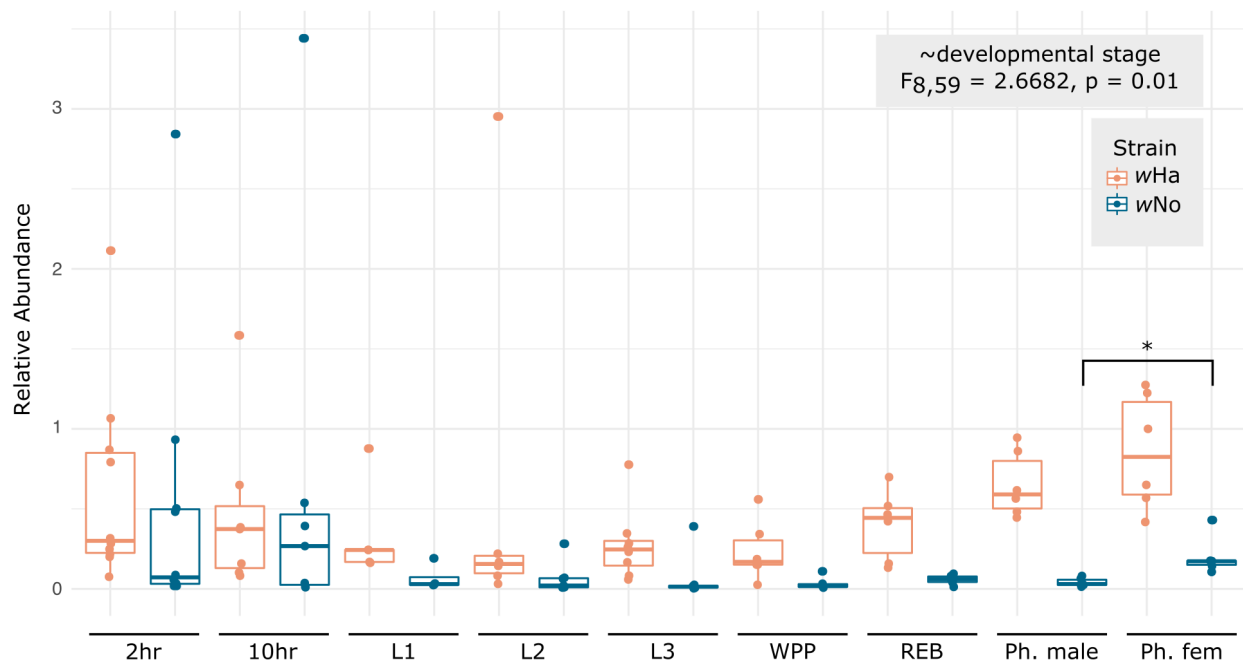
265
266 We then tested for correlation between the relative abundance of *wHa* and *wNo* within a sample
267 type. We found that in ovaries and male carcasses, there was a significant positive correlation
268 between the abundance of *wHa* and *wNo* ($\rho = 0.0238$, $p = 0.8571$, and, $\rho = 0.9643$, $p = 0.0023$,
269 respectively). However, in testes and female carcasses, titers of *wHa* and *wNo* were uncorrelated
270 ($\rho = 0.0714$, $p = 0.9063$, and $\rho = 0.5357$, $p = 0.2357$, respectively). Next, we asked if there
271 was any correlation in the coinfection between samples that originated from the same fly. We did
272 this in two ways: (1) by comparing the ratio of *wHa* and *wNo* within the gonads, to the same ratio
273 in the carcass, and (2) by comparing the total abundance of *wHa* and *wNo* between gonads and
274 carcass. In both cases, we found no significant relationship between the infection dynamics in the
275 gonads and the carcass (Supplemental Figure S1). In fact, female flies had a very consistent ratio
276 of *wHa* to *wNo* in the ovaries (0.39 ± 0.1) and highly variable *wHa:wNo* ratios in the carcass
277 (6.08 ± 4.69). In agreement with the data shown in Figure 2B, the opposite is true in males: the
278 *wHa:wNo* ratio is more consistent in the carcass, but highly variable in the testes (Supplemental
279 Fig S1).

280

281 The coinfection is dynamic across development

282 Given the difference in coinfection between sexes and tissues, we wondered if this was due to
283 differences in transmission of *Wolbachia* to embryos and/or changes across development. To test
284 this, we set up timed egg-lays and collected a developmental series that included seven

285 timepoints across development (from 2-hour old embryos to red-eye-bald pupal stage) as well as
286 newly emerged pharate males and females (Figure 3). Strain-specific qPCR revealed that the
287 coinfection changed significantly across development (Figure 3; $F_{8,59} = 2.6682$, $p = 0.01$). Note
288 that juvenile stages were collected without regard to sex, but there were no indications of bimodal
289 distributions which might indicate that juvenile males and females had drastically different patterns
290 of infection. Notably, the pattern of infection in very young embryos did not resemble any of the
291 previously assessed sample types, including the ovaries. Indeed, 2-hour old embryos had more
292 equal titers of *wHa* and *wNo*, unlike the strong *wNo* bias in ovaries, and unlike the strong *wHa*
293 bias in carcasses and testes. By the first larval instar (L1), the coinfection converged on a pattern
294 more similar to the carcass tissue and testes, where *wHa* titers were much higher than *wNo*. This
295 pattern was relatively stable throughout development. In the newly eclosed pharate females there
296 was a significant increase in *wNo* titer relative to the pharate males ($p = 0.0286$) likely indicative
297 of a shift towards the *wNo* bias we saw in three-day old female ovaries (Figure 2B).



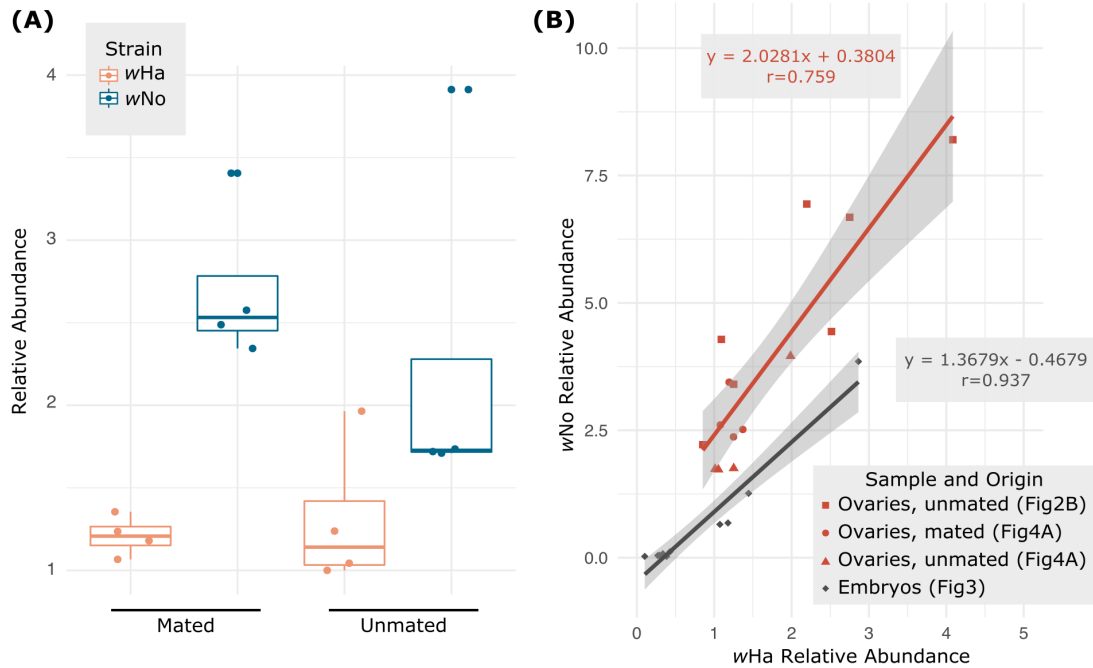
298 **Figure 3. Coinfection is dynamic across development.** Relative abundance of *wHa* and *wNo*
299 across development. Developmental stages include, from left to right, 2-hour old embryos, 10-
300

301 hour old embryos, 1st instar larvae (L1), 2nd instar larvae (L2), 3rd instar larvae (L3), white
302 prepupae (WPP), red-eye bald pupal stage (REB), pharate (Ph.) males, and Ph. females.

303

304 Transmission of the coinfection to embryos is strain-specific

305 The developmental series revealed that very young embryos had coinfections that were dissimilar
306 to the infections in ovaries which raises questions about how the two *Wolbachia* are transmitted
307 to the next generation (Figure 2B). However, the data presented in Figure 2B were generated
308 from unmated females, so we sought to determine if the coinfection differed due to mating, which
309 might explain why the embryos had differing ratios of the two *Wolbachia* strains. We found no
310 significant difference in the coinfection between ovaries derived from three day-old mated and
311 unmated females, and in both cases *wNo* was significantly higher titer than *wHa* (Figure 4A;
312 ~strain*mated status: $F_{1,12} = 1.055$, $p = 0.3246$; ~mated status: $F_{1,12} = 0.473$, $p = 0.5049$; ~strain:
313 $F_{1,12} = 22.891$, $p = 0.0005$). We then used linear regression to assess the relationship between
314 *wHa* and *wNo* in ovary and embryo samples with an eye towards the transmission dynamics. In
315 both sample types there was a significant positive correlation between *wHa* and *wNo*, (ovaries:
316 $F_{1,13} = 45.13$, $p < 0.0001$, $r = 0.759$; embryos: $F_{1,8} = 133.9$, $p < 0.0001$, $r = 0.937$). However, in
317 ovaries *wNo* was more than double the abundance of *wHa*, whereas the two infections were
318 closer to 1:1 in embryos (Figure 4B; ovaries: $y=2.0281x+0.3804$; embryos: $y=1.3679x-0.4679$).
319 Therefore, transmission to embryos favors *wHa*. This is also seen in the negative intercept along
320 the y-axis (*wNo*), indicating a higher likelihood that embryos might receive only *wHa*, but not *wNo*
321 at especially low levels of overall transmission, even though ovaries contain double the titer of
322 *wNo*.



323

324 **Figure 4. The ratio of wHa and wNo transmitted to embryos is not reflective of the**

325 **coinfection in ovaries. (A)** Titers of wHa and wNo do not significantly change upon mating.

326 Newly eclosed females were collected and a subset were mated after 24-hours. Three days post

327 eclosion, ovaries were dissected from the mated and unmated females. Only strain identity (wHa

328 versus wNo) significantly affected titer (\sim strain*mated status: $F_{1,12} = 1.055$, $p = 0.3246$; \sim mated

329 status: $F_{1,12} = 0.473$, $p = 0.5049$; \sim strain: $F_{1,12} = 22.891$, $p = 0.0005$). (B) wHa and wNo titers are

330 strongly correlated within ovaries, and within embryos. However, the ratios of wHa:wNo are

331 significantly different between the two, indicated by the negative y-intercept (wNo) for embryos

332 as compared to ovaries.

333

334 Heat stress facilitates destabilization of co-transmission

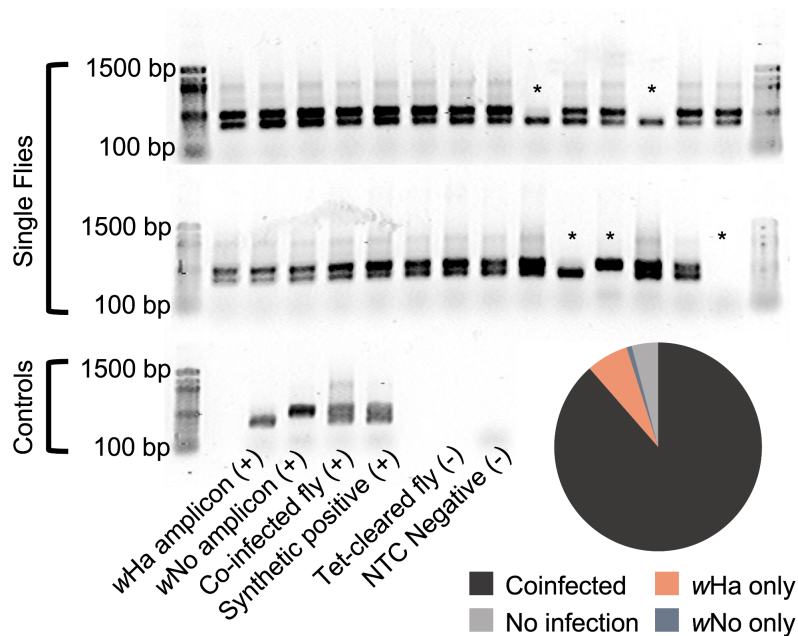
335 We hypothesized that we could perturb the transmission of the coinfection through a heat-

336 mediated reduction in *Wolbachia* titers, which would facilitate a strong bottleneck and the

337 opportunity to isolate individual *Wolbachia* strains. Indeed, subjecting flies to 30 °C for four days

338 resulted in some F1 progeny (11.5%) that were lacking in one or both *Wolbachia* strains (Figure

339 5). This is in contrast to the offspring of flies reared at 25 °C, where the coinfection is stably
340 transmitted: in our routine lab screens we have yet to find flies from this stock that do not carry
341 both infections (n > 200).



342
343 **Figure 5. Heat stress destabilizes co-transmission of wHa and wNo.** Gel electrophoresis of
344 multiplex PCR assay indicating flies that have lost one or both *Wolbachia* infections (*). The
345 “synthetic positive” control was generated by combining previously generated wHa and wNo
346 amplicons in equimolar ratios. Negative controls include flies cleared of their *Wolbachia* infections,
347 and no template controls (NTC). The pie chart summarizing the numbers of flies that lost
348 *Wolbachia* infections (n = total 122 flies screened: wHa only = 8, wNo only = 1, uninfected = 5).

349 350 **DISCUSSION**

351 We hypothesized that stability of multiple *Wolbachia* infections was made possible by some level
352 of niche partitioning. That a coinfection is typically comprised of strains from different
353 supergroups, with each supergroup having a unique set of clade-specific genes (49-51) supports
354 this idea. In wHa and wNo we identified strain-specific proteins predicted to be involved in

355 separate metabolic pathways, as well as proteins that may provide different mechanisms for host
356 interaction and virulence. Indeed, *wHa* and *wNo* have different patterns of tissue tropism across
357 males and females and show different transmission and growth dynamics across fly development.

358

359 While *wHa* and *wNo* titers differed significantly between the ovaries and early embryos, the
360 mechanisms that resulted in differential transmission of *wHa* and *wNo* are still unclear. While *wHa*
361 and *wNo* titers within the ovary are distinct from titers elsewhere in the body, there may be cell-
362 type specificity within the ovary. Ovaries contain a variety of both somatic and germline cell-types,
363 and there are documented examples of cell-type tropisms that also differ across *Wolbachia* strains
364 (52, 53). Strain-specific imaging of whole ovarioles will allow us to determine how each *Wolbachia*
365 strain is distributed within the ovary and in oocytes. The “assembly line” structure of *Drosophila*
366 ovarioles offers a convenient way to capture changes in tissue specificity and titer that occur as
367 eggs mature and may provide an explanation for the discrepancies in composition of the
368 *Wolbachia* community that we see between whole ovaries and embryos.

369

370 After *wHa* and *wNo* are transmitted to the embryos, the coinfection seems to converge on a
371 pattern consisting of a relatively low and stable population of *wNo* and a comparatively high level
372 of *wHa* that persists throughout development. When the adults emerge, we see the first evidence
373 of increasing *wNo* titers in females. Our data suggest that the switch from the high *wHa*:*wNo* ratio
374 seen in juveniles to the relatively equal *wHa*:*wNo* titers of three day old females occurs during
375 adulthood, not metamorphosis. This process may be linked to ovary maturation as an adult rather
376 than imaginal disc differentiation during the pupal period, but more in-depth analyses of the
377 imaginal discs and the adult female maturation period are needed to tease this apart.

378

379 The differences in infection between ovaries and testes raise several questions about the
380 reproductive manipulation induced by these strains: Cytoplasmic Incompatibility (CI). In the

381 testes, CI results in altered sperm that cause embryonic lethality, unless “rescued” by a
382 complementary infection in the oocyte (54). In the case of coinfections, typically each strain-
383 specific alteration of the sperm requires a matching rescue or antidote in the embryo (10, 55), and
384 previous studies indicate that *wHa* and *wNo* are not fully capable of rescuing the other strain’s CI
385 induction (46). These CI induction and rescue processes are mediated by *Wolbachia* “Cif”
386 proteins, and there is strong evidence that the level of Cif expression, and the availability of strain-
387 specific cognate partners is critical for proper induction and rescue (54, 56-59). Given this, it was
388 interesting to find that the ratio of *wHa* to *wNo* within the testes was more variable between
389 individuals than it was across ovaries (in which *wHa* and *wNo* titers were strongly correlated).
390 Additionally, *wHa* was the dominant strain in testes, as compared to *wNo* being dominant in the
391 ovaries. It is not clear if the ratios of *wHa* and *wNo* infections in the gonad tissues are reflective
392 of the level of Cif proteins in gametes, and ultimately the level of induction and rescue caused by
393 each strain. Perhaps expression and deposition of Cif proteins is regulated in a cell-type-specific
394 or co-infection sensitive manner. Finally, we do not know if CI rescue is oocyte-autonomous, or if
395 Cif proteins are transported between cell types (e.g., from somatic follicle cells to the oocyte).
396 Which cell types do *Wolbachia* need to be in, and at what time points in gametogenesis in order
397 to cause or rescue CI? Perhaps the quantity of Cif proteins from each strain that are deposited in
398 spermatozoa and oocytes are tightly regulated such that they more closely mirror each other. A
399 combination of molecular approaches to assess Cif protein abundance in gametes, combined
400 with genetic tools to test for cell autonomy will be useful for understanding these processes, and
401 ultimately how CI is regulated.

402

403 Finally, we demonstrated that heat stress disrupts vertical transmission of *wHa* and *wNo* through
404 an unknown mechanism. We hypothesize that heat stress negatively impacts *Wolbachia* titers
405 (60), causing the bacteria to be “diluted” as cells in the ovary chain divide. In rare instances, a
406 developing oocyte will receive *Wolbachia* of only one strain or no *Wolbachia* at all. Using a heat

407 treatment, we recovered more flies that only had the *wHa* strain (and had lost *wNo*), and only one
408 example of a fly that only had *wNo* ($n = 1$). This may be due to the preferential transmission of
409 *wHa* that we saw when comparing ovary and embryo coinfections, or potentially strain-specific
410 differences in heat-sensitivity. Indeed, a recent study showed that temperature is a strong driver
411 of *Wolbachia* transmission and spread at large scales (61), and there are many other examples
412 of high temperatures that result in full or partial cures of *Wolbachia* (60). Our ability to segregate
413 the strains into mono-infections in the same genomic background will be a useful tool for exploring
414 the strain-specific contributions to host physiology, and for understanding the interactions
415 between coinfecting *Wolbachia*. Indeed, a combination of factors likely governs *Wolbachia*
416 community dynamics, and it is unclear if *wHa* and *wNo* interactions with each other are
417 competitive, synergistic, or perhaps parasitic. Disentangling the relative contributions of each
418 strain to the stability of the coinfection will inform efforts to establish multiple infections of selected
419 symbionts and contribute to understanding the dynamics of the intracellular community more
420 broadly.

421

422

423

424

425

426

427

428

429

430

431

432

433 **DECLARATIONS**

434 Acknowledgements

435 This work was supported by UMN AGREETT startup funds to ARIL. Many thanks to Brandon
436 Cooper for gifting us the *Drosophila simulans* stock. LCF was supported by UMN DOVE and UMN
437 CFANS Match fellowships. MWJ was supported by an Excellence in Entomology Fellowship from
438 UMN.

439

440 Conflicts of interest

441 The authors declare that they have no competing interests.

442

443 Data Availability

444 **Supplemental File S1.** Contains supplemental figures.

445 **Figure S1.** Within-fly gonad and carcass infection dynamics.

446 **Figure S2.** *w*Ha and *w*No correlation across development.

447 **Supplemental File S2:** Contains supplemental tables. Metadata are in the first tab of the file.

448 **Table S1.** FtsZ protein accession numbers used for phylogenetic reconstruction.

449 **Table S2.** KEGG annotations for *w*Ha and *w*No specific proteins.

450 **Tables S3-S7.** qPCR data by figure.

451

452

453

454

455

456

457

458

459 **TABLES**

460 **Table 1.** Primer sequences used in this study.

Assay Target	Primer	Sequence (5' - 3')	Reference
<i>wsp</i> multiplex	81F	TGGTCCAATAAGTGATGAAGAAAC	(James <i>et al</i> , 2002)
	463R	TACCATTTTGACTACTCACAGCG	
	635R	GATCTCTTTAGTAGCTGATAC	
Arthropod 28S	28S_F	CCCTGTTGAGCTTGACTCTAGTCTGGC	(Werren <i>et al</i> , 1995)
	28S_R	AAGAGCCGACATCGAAGGATC	
<i>wHa wsp</i> qPCR	<i>wsp_wHa_qPCR_F</i>	AAAGAAGACTGCGGATACTGAT	This study
	<i>wsp_wHa_qPCR_R</i>	CTGCGAATAAAGCCCTTCAAC	
<i>wNo wsp</i> qPCR	<i>wsp_wNo_qPCR_F</i>	CAGCAATCCTTCAGAAGCTAGT	This study
	<i>wsp_wNo_qPCR_R</i>	AAATAACGAGCACCAGCATAAAG	
<i>D. simulans rpl32</i> qPCR	<i>rpl32_Dsim_qPCR_F</i>	AGGGTATCGACAACAGAGTG	This study
	<i>rpl32_Dsim_qPCR_R</i>	GGAACTTCTTGAATCCGGTG	

461

462

463

464

465

466

467

468

469

470

471

472

473

474

475

476

477

478

479 **REFERENCES**

- 480 1. Duron O, Bouchon D, Boutin S, Bellamy L, Zhou L, Engelstädter J, Hurst GD. 2008. The
481 diversity of reproductive parasites among arthropods: *Wolbachia* do not walk alone. BMC
482 Biol 6:1-12.
- 483 2. Duron O, Hurst GD. 2013. Arthropods and inherited bacteria: from counting the symbionts
484 to understanding how symbionts count. BMC Biol 11:1-4.
- 485 3. Dumler JS, Barbet AF, Bekker C, Dasch GA, Palmer GH, Ray SC, Rikihisa Y, Rurangirwa
486 FR. 2001. Reorganization of genera in the families Rickettsiaceae and Anaplasmataceae
487 in the order Rickettsiales: unification of some species of *Ehrlichia* with *Anaplasma*,
488 *Cowdria* with *Ehrlichia* and *Ehrlichia* with *Neorickettsia*, descriptions of six new species
489 combinations and designation of *Ehrlichia equi* and 'HGE agent' as subjective synonyms of
490 *Ehrlichia phagocytophila*. Int J Syst Evol Microbiol 51:2145-2165.
- 491 4. Werren JH, Baldo L, Clark ME. 2008. *Wolbachia*: master manipulators of invertebrate
492 biology. Nat Rev Micro 6:741-751.
- 493 5. Kaur R, Shropshire JD, Cross KL, Leigh B, Mansueto AJ, Stewart V, Bordenstein SR,
494 Bordenstein SR. 2021. Living in the endosymbiotic world of *Wolbachia*: A centennial
495 review. Cell Host & Microbe.
- 496 6. Werren JH, Windsor D, Guo LR. 1995. Distribution of *Wolbachia* among neotropical
497 arthropods. Proc R Soc Lond B 262:197-204.
- 498 7. Bordenstein SR, Werren JH. 1998. Effects of A and B *Wolbachia* and host genotype on
499 interspecies cytoplasmic incompatibility in *Nasonia*. Genetics 148:1833-1844.
- 500 8. Ellegaard KM, Klasson L, Naslund K, Bourtzis K, Andersson SGE. 2013. Comparative
501 genomics of *Wolbachia* and the bacterial species concept. PLoS Genet 9:e1003381.
- 502 9. Dutton TJ, Sinkins SP. 2004. Strain-specific quantification of *Wolbachia* density in *Aedes*
503 *albopictus* and effects of larval rearing conditions. Insect Mol Biol 13:317-322.

- 504 10. Dobson S, Rattanadechakul W, Marsland E. 2004. Fitness advantage and cytoplasmic
505 incompatibility in *Wolbachia* single-and superinfected *Aedes albopictus*. *Heredity* 93:135-
506 142.
- 507 11. Bordenstein SR, O'hara FP, Werren JH. 2001. *Wolbachia*-induced incompatibility
508 precedes other hybrid incompatibilities in *Nasonia*. *Nature* 409:707-710.
- 509 12. Merçot H, Poinso D. 1998. *Wolbachia* transmission in a naturally bi-infected *Drosophila*
510 *simulans* strain from New-Caledonia. *Entomol Exp Appl* 86:97-103.
- 511 13. Kent BN, Salichos L, Gibbons JG, Rokas A, Newton ILG, Clark ME, Bordenstein SR. 2011.
512 Complete bacteriophage transfer in a bacterial endosymbiont (*Wolbachia*) determined by
513 targeted genome capture. *Genome Biol Evol* 3:209-218.
- 514 14. Chafee ME, Funk DJ, Harrison RG, Bordenstein SR. 2010. Lateral phage transfer in
515 obligate intracellular bacteria (*Wolbachia*): verification from natural populations. *Mol Biol*
516 *Evol* 27:501-5.
- 517 15. Baldo L, Bordenstein S, Wernegreen JJ, Werren JH. 2006. Widespread recombination
518 throughout *Wolbachia* genomes. *Mol Biol Evol* 23:437-449.
- 519 16. Lindsey ARI, Bhattacharya T, Newton ILG, Hardy RW. 2018. Conflict in the intracellular
520 lives of endosymbionts and viruses: A mechanistic look at *Wolbachia*-mediated pathogen-
521 blocking. *Viruses* 10:141.
- 522 17. Joubert DA, Walker T, Carrington LB, De Bruyne JT, Kien DHT, Hoang NLT, Chau NVV,
523 Iturbe-Ormaetxe I, Simmons CP, O'Neill SL. 2016. Establishment of a *Wolbachia*
524 superinfection in *Aedes aegypti* mosquitoes as a potential approach for future resistance
525 management. *PLoS Path* 12:e1005434.
- 526 18. Ross PA, Turelli M, Hoffmann AA. 2019. Evolutionary ecology of *Wolbachia* releases for
527 disease control. *Annu Rev Genet* 53:93-116.
- 528 19. Walker T, Johnson PH, Moreira LA, Iturbe-Ormaetxe I, Frentiu FD, McMeniman CJ, Leong
529 YS, Dong Y, Axford J, Kriesner P, Lloyd AL, Ritchie SA, O'Neill SL, Hoffmann AA. 2011.

- 530 The wMel *Wolbachia* strain blocks dengue and invades caged *Aedes aegypti* populations.
531 Nature 476:450-U101.
- 532 20. Hoffmann AA, Montgomery BL, Popovici J, Iturbe-Ormaetxe I, Johnson PH, Muzzi F,
533 Greenfield M, Durkan M, Leong YS, Dong Y, Cook H, Axford J, Callahan AG, Kenny N,
534 Omodei C, McGraw EA, Ryan PA, Ritchie SA, Turelli M, O'Neill SL. 2011. Successful
535 establishment of *Wolbachia* in *Aedes* populations to suppress dengue transmission.
536 Nature 476:454-U107.
- 537 21. Hoffmann AA, Ross PA, Rasic G. 2015. *Wolbachia* strains for disease control: ecological
538 and evolutionary considerations. Ecol Evol 8:751-68.
- 539 22. Black C, Bermudez L, Young L, Remington J. 1990. Co-infection of macrophages
540 modulates interferon gamma and tumor necrosis factor-induced activation against
541 intracellular pathogens. The Journal of Experimental Medicine 172:977-980.
- 542 23. Erickson AK, Jesudhasan PR, Mayer MJ, Narbad A, Winter SE, Pfeiffer JK. 2018. Bacteria
543 facilitate enteric virus co-infection of mammalian cells and promote genetic recombination.
544 Cell Host & Microbe 23:77-88. e5.
- 545 24. Nakamura S, Davis KM, Weiser JN. 2011. Synergistic stimulation of type I interferons
546 during influenza virus coinfection promotes *Streptococcus pneumoniae* colonization in
547 mice. J Clin Invest 121.
- 548 25. Spier A, Stavru F, Cossart P. 2019. Interaction between intracellular bacterial pathogens
549 and host cell mitochondria. Bacteria and Intracellularity:1-13.
- 550 26. Heddi A, Grenier A-M, Khatchadourian C, Charles H, Nardon P. 1999. Four intracellular
551 genomes direct weevil biology: nuclear, mitochondrial, principal endosymbiont, and
552 *Wolbachia*. Proc Natl Acad Sci 96:6814-6819.
- 553 27. Sassera D, Beninati T, Bandi C, Bouman EA, Sacchi L, Fabbi M, Lo N. 2006. '*Candidatus*
554 *Midichloria mitochondrii*', an endosymbiont of the tick *Ixodes ricinus* with a unique
555 intramitochondrial lifestyle. Int J Syst Evol Microbiol 56:2535-2540.

- 556 28. Ramírez-Puebla ST, Ormeño-Orrillo E, Vera-Ponce de León A, Lozano L, Sanchez-Flores
557 A, Rosenblueth M, Martínez-Romero E. 2016. Genomes of *Candidatus Wolbachia*
558 *bourtzisii* w DacA and *Candidatus Wolbachia pipientis* w DacB from the Cochineal Insect
559 *Dactylopius coccus* (Hemiptera: Dactylopiidae). *G3: Genes, Genomes, Genetics* 6:3343-
560 3349.
- 561 29. Liang X, Liu J, Bian G, Xi Z. 2020. *Wolbachia* inter-strain competition and inhibition of
562 expression of cytoplasmic incompatibility in mosquito. *Frontiers in Microbiology* 11:1638.
- 563 30. Kang L, Ma X, Cai L, Liao S, Sun L, Zhu H, Chen X, Shen D, Zhao S, Li C. 2003.
564 Superinfection of *Laodelphax striatellus* with *Wolbachia* from *Drosophila simulans*.
565 *Heredity* 90:71-76.
- 566 31. Rousset F, Braig HR, O'Neill SL. 1999. A stable triple *Wolbachia* infection in *Drosophila*
567 with nearly additive incompatibility effects. *Heredity* 82:620-627.
- 568 32. Walker T, Song S, Sinkins SP. 2009. *Wolbachia* in the *Culex pipiens* group mosquitoes:
569 introgression and superinfection. *J Hered* 100:192-196.
- 570 33. Ant TH, Sinkins SP. 2018. A *Wolbachia* triple-strain infection generates self-incompatibility
571 in *Aedes albopictus* and transmission instability in *Aedes aegypti*. *Parasites & Vectors*
572 11:1-7.
- 573 34. Schneider DI, Riegler M, Arthofer W, Merçot H, Stauffer C, Miller WJ. 2013. Uncovering
574 *Wolbachia* diversity upon artificial host transfer. *PLoS One* 8:e82402.
- 575 35. Fu Y, Gavotte L, Mercer DR, Dobson SL. 2010. Artificial triple *Wolbachia* infection in
576 *Aedes albopictus* yields a new pattern of unidirectional cytoplasmic incompatibility. *Appl*
577 *Environ Microbiol* 76:5887-5891.
- 578 36. Osborne SE, Leong YS, O'Neill SL, Johnson KN. 2009. Variation in antiviral protection
579 mediated by different *Wolbachia* strains in *Drosophila simulans*. *PLoS Path* 5:e1000656.

- 580 37. Osborne SE, Iturbe-Ormaetxe I, Brownlie JC, O'Neill SL, Johnson KN. 2012. Antiviral
581 protection and the importance of *Wolbachia* density and tissue tropism in *Drosophila*
582 *simulans*. *Appl Environ Microbiol* 78:6922-6929.
- 583 38. Poinot D, Montchamp-Moreau C, Merçot H. 2000. *Wolbachia* segregation rate in
584 *Drosophila simulans* naturally bi-infected cytoplasmic lineages. *Heredity* 85:191-198.
- 585 39. Mouton L, Dedeine F, Henri H, Boulétreau M, Profizi N, Vavre F. 2004. Virulence, multiple
586 infections and regulation of symbiotic population in the *Wolbachia-Asobara tabida*
587 symbiosis. *Genetics* 168:181-189.
- 588 40. Mouton L, Henri H, Bouletreau M, Vavre F. 2003. Strain-specific regulation of intracellular
589 *Wolbachia* density in multiply infected insects. *Mol Ecol* 12:3459-3465.
- 590 41. Tatusova T, DiCuccio M, Badretdin A, Chetvernin V, Nawrocki EP, Zaslavsky L, Lomsadze
591 A, Pruitt KD, Borodovsky M, Ostell J. 2016. NCBI prokaryotic genome annotation pipeline.
592 *Nucleic Acids Res* 44:6614-6624.
- 593 42. Lechner M, Findeiß S, Steiner L, Marz M, Stadler PF, Prohaska SJ. 2011. Proteinortho:
594 detection of (co-) orthologs in large-scale analysis. *BMC Bioinformatics* 12:1-9.
- 595 43. Kanehisa M, Sato Y, Morishima K. 2016. BlastKOALA and GhostKOALA: KEGG tools for
596 functional characterization of genome and metagenome sequences. *J Mol Biol* 428:726-
597 731.
- 598 44. Katoh K, Rozewicki J, Yamada KD. 2019. MAFFT online service: multiple sequence
599 alignment, interactive sequence choice and visualization. *Briefings in Bioinformatics*
600 20:1160-1166.
- 601 45. Bhattacharya T, Newton ILG, Hardy RW. 2017. *Wolbachia* elevates host
602 methyltransferase expression to block an RNA virus early during infection. *PLoS Path*
603 13:e1006427.
- 604 46. James A, Dean M, McMahon M, Ballard J. 2002. Dynamics of double and single
605 *Wolbachia* infections in *Drosophila simulans* from New Caledonia. *Heredity* 88:182-189.

- 606 47. R Core Team. 2014. R: A language and environment for statistical computing, URL
607 <http://www.R-project.org/>, R Foundation for Statistical Computing, Vienna, Austria.
- 608 48. Oksanen J, Blanchet FG, Kindt R, Legendre P, Minchin PR, O'Hara R, Simpson GL,
609 Solymos P, Stevens M, Wagner H. 2015. *vegan*: Community Ecology Package. R
610 package version 2.0-1. <http://CRANR-projectorg/package=vegan>.
- 611 49. Lindsey ARI, Werren JH, Richards S, Stouthamer R. 2016. Comparative genomics of a
612 parthenogenesis-inducing *Wolbachia* symbiont. *G3: Genes|Genomes|Genetics* 6:2113-
613 2123.
- 614 50. Lindsey ARI. 2020. Sensing, Signaling, and Secretion: A review and analysis of systems
615 for regulating host interaction in *Wolbachia*. *Genes* 11:813.
- 616 51. Rice DW, Sheehan KB, Newton IL. 2017. Large-scale identification of *Wolbachia pipientis*
617 effectors. *Genome Biol Evol* 9:1925-1937.
- 618 52. Fast EM, Toomey ME, Panaram K, Desjardins D, Kolaczyk ED, Frydman HM. 2011.
619 *Wolbachia* enhance *Drosophila* stem cell proliferation and target the germline stem cell
620 niche. *Science* 334:990-992.
- 621 53. Frydman HM, Li JM, Robson DN, Wieschaus E. 2006. Somatic stem cell niche tropism in
622 *Wolbachia*. *Nature* 441:509-12.
- 623 54. Beckmann JF, Bonneau M, Chen H, Hochstrasser M, Poinot D, Merçot H, Weill M, Sicard
624 M, Charlat S. 2019. The toxin–antidote model of cytoplasmic incompatibility: genetics and
625 evolutionary implications. *Trends Genet.*
- 626 55. Sinkins S, Braig H, O'Neill SL. 1995. *Wolbachia* superinfections and the expression of
627 cytoplasmic incompatibility. *Proceedings of the Royal Society of London Series B:*
628 *Biological Sciences* 261:325-330.
- 629 56. Shropshire JD, Bordenstein SR. 2019. Two-By-One model of cytoplasmic incompatibility:
630 Synthetic recapitulation by transgenic expression of *cifA* and *cifB* in *Drosophila*. *PLoS*
631 *Genet* 15.

- 632 57. Chen H, Ronau JA, Beckmann JF, Hochstrasser M. 2019. A *Wolbachia* nuclease and its
633 binding partner provide a distinct mechanism for cytoplasmic incompatibility. Proc Natl
634 Acad Sci 116:22314-22321.
- 635 58. Lindsey ARI, Rice DW, Bordenstein SR, Brooks AW, Bordenstein SR, Newton ILG. 2018.
636 Evolutionary genetics of cytoplasmic incompatibility genes *cifA* and *cifB* in prophage WO
637 of *Wolbachia*. Genome Biol Evol 10:434-451.
- 638 59. Beckmann JF, Ronau JA, Hochstrasser M. 2017. A *Wolbachia* deubiquitylating enzyme
639 induces cytoplasmic incompatibility. Nat Micro 2:17007.
- 640 60. López-Madrigal S, Duarte EH. 2019. Titer regulation in arthropod-*Wolbachia* symbioses.
641 FEMS Microbiol Lett 366:fnz232.
- 642 61. Hague MT, Shropshire JD, Caldwell CN, Statz JP, Stanek KA, Conner WR, Cooper BS.
643 2022. Temperature effects on cellular host-microbe interactions explain continent-wide
644 endosymbiont prevalence. Curr Biol 32:878-888. e8.
- 645